RNA–Protein Complexes

DOI: 10.1002/ange.201405362

Uncovering the Stoichiometry of *Pyrococcus furiosus* RNase P, a Multi-Subunit Catalytic Ribonucleoprotein Complex, by Surface-Induced Dissociation and Ion Mobility Mass Spectrometry**

Xin Ma, Lien B. Lai, Stella M. Lai, Akiko Tanimoto, Mark P. Foster, Vicki H. Wysocki, and Venkat Gopalan**

Abstract: *We demonstrate that surface-induced dissociation (SID) coupled with ion mobility mass spectrometry (IM-MS) is a powerful tool for determining the stoichiometry of a multi-subunit ribonucleoprotein (RNP) complex assembled in a solution containing Mg^{2+}. We investigated Pyrococcus furiosus (Pfu) RNase P, an archaeal RNP that catalyzes tRNA 5′ maturation. Previous step-wise, Mg^{2+}-dependent reconstitutions of Pfu RNase P with its catalytic RNA subunit and two interacting protein cofactor pairs (RPP21·RPP29 and POP5·RPP30) revealed functional RNP intermediates en route to the RNase P enzyme, but provided no information on subunit stoichiometry. Our native MS studies with the proteins showed RPP21·RPP29 and $(POP5{\cdot}RPP30)_2$ complexes, but indicated a 1:1 composition for all subunits when either one or both protein complexes bind the cognate RNA. These results highlight the utility of SID and IM-MS in resolving conformational heterogeneity and yielding insights on RNP assembly.*

Nanoelectrospray ionization-based native mass spectrometry (MS) has been used to determine the stoichiometry, structure, and interactions of several noncovalent protein assemblies, including large viral capsids (10^6 Da range),[1] but its use has been restricted to only a few ribonucleoprotein (RNP) complexes assembled without divalent cations.[1c,2] The limited progress with RNPs is partly due to the weak signal intensity and poor resolution caused by ionization suppression[3] and peak broadening,[4] respectively; both are inevitable consequences of the nonspecific attachment of nonvolatile cations (e.g., Mg^{2+}) required for the assembly of many cellular RNPs. Additionally, the volatile buffers (e.g., ammonium acetate)[5] that are typically used to promote formation of analyte ions in native MS may not be ideal for forming the functionally relevant RNP complex. To overcome these challenges, it is critical to isolate low abundance ionic species and identify their subunit make-up. Here, we demonstrate how tandem MS (MS/MS) and ion mobility (IM), which have already provided information about the architecture and dynamics of protein complexes,[1a–e,g-i,6] can also be used in combination with surface-induced dissociation (SID) to resolve RNP heterogeneity and to determine the stoichiometry of archaeal RNase P, a multi-subunit RNP.

In all organisms, RNase P is an essential enzyme that cleaves the 5′-leader of precursor tRNAs (pre-tRNAs) in a Mg^{2+}-dependent manner to yield functional mature tRNAs.[7–9] Whereas an RNA-free, protein-based form of RNase P has been reported in several eukaryotes,[8] the RNP form is found in all domains of life. The RNP form comprises a catalytic RNase P RNA (RPR) and a variable number of RNase P proteins (RPPs) depending on the source: one in bacteria, up to five in archaea, and as many as ten in eukaryotes.[7,9] A common ancestry for all RPRs is evident in their highly conserved sequences and structural elements, but sequence similarity for RPPs is shared only between archaea and eukaryotes. Whereas eukaryotic RNase P has not been reconstituted in vitro, RNase P from several archaea has been assembled from recombinant RPR and RPPs.[10] High-resolution structures of archaeal RPPs have also been determined.[9a,11] These advances make archaeal RNase P an attractive experimental model for understanding how multiple proteins modulate the structure, dynamics, and function of an RNA in a large RNP, while serving as a tractable surrogate for its eukaryotic relative.

In our biochemical studies on RNase P from the archaeon *Pyrococcus furiosus* (*Pfu*), we determined that the addition of the four RPPs to the RPR leads to a 4250-fold enhancement of its k_{cat}/K_M and that the RPPs function as binary complexes (RPP21·RPP29 and POP5·RPP30).[10d] The assembly of the RPR with each binary complex is functional, albeit only at higher concentrations of Mg^{2+} (120 instead of 30 mM) and with a lower k_{cat}/K_M than that of the RNP reconstituted with both pairs.[10a,d] These findings were presaged and subsequently confirmed by genetic and structural studies. First, yeast two-hybrid analysis of *Methanothermobacter thermautotrophicus* and *Pyrococcus horikoshii (Pho)* RPPs showed strong interactions between RPP21 and RPP29 as well as between POP5 and RPP30.[12] Second, RPP21 and RPP29 were found by X-ray crystallography and NMR spectroscopy to interact as a heterodimer.[11a,d] Third, the crystal structure of POP5 and RPP30 from *Pho* revealed a heterotetramer with a POP5 dimer placed between two RPP30 monomers.[11b]

[*] X. Ma,[+] L. B. Lai,[+] S. M. Lai,[+] A. Tanimoto, Prof. M. P. Foster, Prof. V. H. Wysocki, Prof. V. Gopalan
Department of Chemistry and Biochemistry
Center for RNA Biology, The Ohio State University
Columbus, OH 43210 (USA)
E-mail: wysocki.11@osu.edu
gopalan.5@osu.edu

[+] These authors contributed equally to this work.

[**] Funding support from the NSF (MCB-0843543 and DBI-0923551) and the NIH (RO1 GM067807) is gratefully acknowledged.

Supporting information for this article is available on the WWW under http://dx.doi.org/10.1002/anie.201405362.

Dynamic light scattering, NMR line widths, and hydrodynamic measurements corroborated a similar $(POP5{\cdot}RPP30)_2$ assembly in *Pfu*.[11c,13] Although comparable studies were not performed on the binary RPPs complexed with the RPR, these results led to some speculations about RNase P assembly, like the idea of *Pho* RNase P comprising two copies each of the RPR and RPPs, centered around a $(POP5{\cdot}RPP30)_2$ heterotetramer flanked symmetrically by two copies of RPP21·RPP29.[11b]

While isotope-coded tags, two-dimensional gel electrophoresis with fluorescent staining, metabolic labeling (SILAC), chemical labeling (iTRAQ), and label-free spectral counts have been employed in MS-based studies to establish the protein composition and stoichiometry of stage-specific spliceosomal RNP complexes,[14] here we have used SID and IM-MS to simultaneously determine the RNA and protein stoichiometry of *Pfu* RNase P. In IM-MS, ions are driven by an electric field to pass through a drift tube filled with bath gas, and those with large collisional cross sections (CCS) and low charge states are slowed down more by the bath gas compared to ions with small CCS and high charge states.[1-h,i,6b,c,15] IM can thus assist in resolving complicated spectra because it can separate ions with the same m/z but different drift times based on differences in charge states, sizes and shapes. Ion source activation and collision-induced dissociation (CID) have been used to remove solvents, salts, and detergents attached to protein ions in the gas phase;[16] we have also employed this collision-induced cleaning technique to remove Mg^{2+} attached nonspecifically to RNAs and RNPs. Because Mg^{2+} can stabilize protein and RNP complexes[17] and create structures that are difficult for CID to break apart, SID was used to dissociate RNPs in the presence of Mg^{2+}. SID deposits high energy into the ions through a single collision event with a surface[18] to reveal dissociation pathways with high energy barriers and high rates, which are likely for RNP disassembly. In tandem with IM, SID can be employed to dissociate a putative RNP complex, thereby confirming its identity and revealing substructures. Together, these MS techniques allowed us to determine a 1:1 composition for all subunits and discern a possible assembly pathway for *Pfu* RNase P reconstituted in the presence of Mg^{2+} from recombinant RPR, RPP21·RPP29, and POP5·RPP30. (See the Supporting Information for a comment on the fifth archaeal RPP.)

To ascertain whether the structures of the RPP complexes observed previously by X-ray crystallography and NMR are preserved in the gas phase, we performed native MS on *Pfu* RPP21·RPP29 and POP5·RPP30. The spectra indeed confirm an RPP21·RPP29 heterodimer and a $(POP5{\cdot}RPP30)_2$ heterotetramer in 500 mM NH_4OAc (Figure 1) as well as in 100 mM and 800 mM (not shown), and provide a reference for their RPR-bound states in the experiments described below.

A major challenge in determining the stoichiometry of RNP complexes such as archaeal RNase P is the optimization of experimental conditions for MS that also closely reflect the native functional state. We focused our initial attention on *Pfu* RPR reconstituted with all four RPPs, a complex that exhibits maximal pre-tRNA cleavage activity in 50 mM Tris-HCl or HEPES-KOH (pH 7.5–8), 800 mM NH_4OAc, and 30 mM $MgCl_2$.[10a,d] Because Tris/HEPES and 30 mM $MgCl_2$ complicate MS experiments, we assembled *Pfu* RPR, RPP21·RPP29, and POP5·RPP30 in 800 mM NH_4OAc and systematically explored a lower $Mg(OAc)_2$ range (2–10 mM). In addition, we found that a careful optimization of the acceleration voltage during collision-induced cleaning was critical to achieve distinguishable RNP signals (Figure S1).

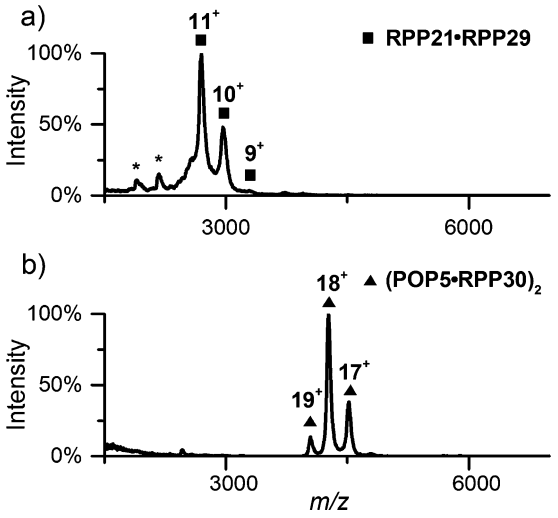

Figure 1. Native MS spectra of *Pfu* RPP21·RPP29 heterodimer (a) and $(POP5{\cdot}RPP30)_2$ heterotetramer (b) in 500 mM NH_4OAc. In each spectrum, the dominant peaks and charge states are indicated. Asterisks indicate the 7^+ and 8^+ states of uncomplexed RPP29, a small amount likely generated from the binary complex during storage or analysis. See Table S1 for predicted and observed masses.

We empirically determined that assembling *Pfu* RPR, RPP21·RPP29, and POP5·RPP30 in 800 mM NH_4OAc and ≤ 3 mM $Mg(OAc)_2$ yielded the best MS data (Figure 2), though there is no evidence of protein aggregation at ≥ 3 mM Mg^{2+}. Whereas the overall RNP stoichiometry and oligomeric state remain the same with either 2 or 3 mM $Mg(OAc)_2$, the data as expected are superior with 2 mM. Figure 2a shows the spectrum for the RPR in 2 mM $Mg(OAc)_2$, observed in the positive-ion mode due to bound Mg^{2+}. Heterogeneous Mg^{2+} complexation in the RPR can also cause peak broadening, leading to the high background signal in the m/z range (6800 to 8200) of the RPR spectrum. When the RPR was assembled with the four proteins in 2 mM $Mg(OAc)_2$, two series of peaks were observed (Figure 2b). The first set of peaks corresponds to the RPR, mirroring the charge states observed with the RPR alone (Figure 2a), while the second matches an RPR bound to one copy of each RPP, an unexpected but informative result given the $(POP5{\cdot}RPP30)_2$ heterotetrameric structure observed in the absence of the RPR (Figure 1). Although of poorer spectral quality, the 4-RPP *Pfu* RNase P complex in 3 mM $Mg(OAc)_2$ also shows a 1:1 composition for all subunits (Figure 2c).

To further confirm the composition of the RNP complex (Figure 2b), CID and SID were employed. Because the signal intensity of the RNP complexes is too low to select a particular peak for dissociation, we chose to dissociate the complexes in the high m/z range (>6400). While even the highest CID acceleration voltage (200 V) did not dissociate the complex

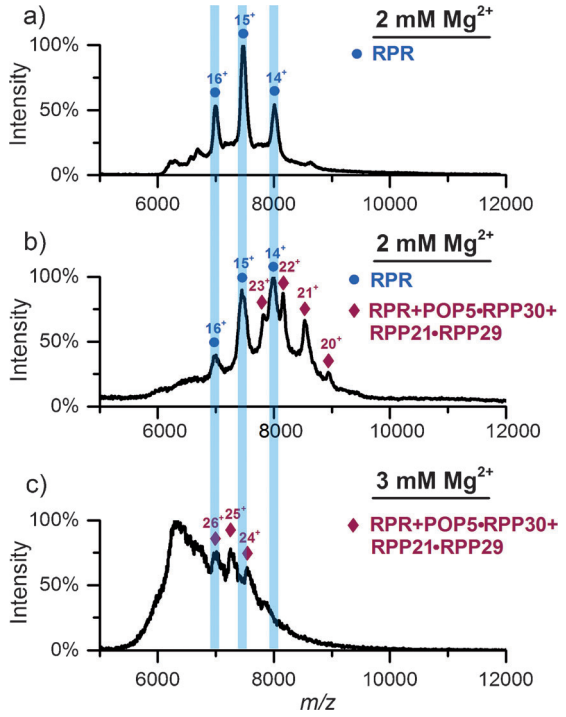

Figure 2. a) *Pfu* RPR in 800 mM NH_4OAc and 2 mM $Mg(OAc)_2$, observed in positive-ion mode. b) RPR, RPP21·RPP29, and POP5·RPP30 in 800 mM NH_4OAc and 2 mM $Mg(OAc)_2$. Peaks corresponding to RPR alone (blue bars) and RPR with one copy of each of the four RPPs are indicated. c) Same as (b) except with 3 mM $Mg(OAc)_2$. Collision-induced cleaning in the first collision cell was optimized to improve peak quality in each case [70 V (a); 130 V (b); 90 V (c); collision energy is V×charge state]. See Table S1 for predicted and observed masses.

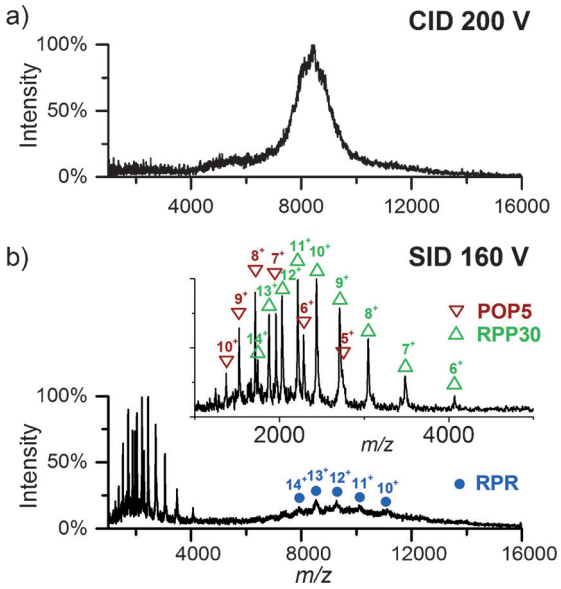

Figure 3. CID and SID of ions in the high *m/z* range (>6400) present in the assembly of RPR, RPP21·RPP29, and POP5·RPP30 in 800 mM NH_4OAc and 2 mM $Mg(OAc)_2$. a) CID at 200 V (4000 to 4600 eV), the highest acceleration voltage possible with the instrument used, did not dissociate the RNP complex. b) SID of precursor (whole charge state envelope) at 160 V (3200–3680 eV) successfully dissociated the RNP complex to produce POP5 and RPP30 monomers as well as the RPR (in the *m/z* range 8000–11000).

(Figure 3a), SID produced RPR, POP5, and RPP30 fragments, validating their presence in the parental RNP (Figure 3b). By subtractive analysis, one can also deduce the presence of RPP21 and RPP29 in the precursor ion: the mass of the complex minus the mass sum of RPR + POP5·RPP30 equals the mass of RPP21·RPP29 (Table S1). These data highlight the previously unproven ability of SID in dissociating Mg^{2+}-stabilized RNP complexes.

We next investigated whether the 4-RPP *Pfu* RNase P complex is functional under the conditions employed for native MS. Because the 2 and 3 mM $Mg(OAc)_2$ used in the MS studies are well below the reported optimum of 30 mM,[10d] we used single-turnover conditions (i.e., $[E] \gg [S]$) to facilitate a qualitative comparison. Whether we assembled *Pfu* RPR, RPP21·RPP29, and POP5·RPP30 in 800 mM NH_4OAc and 2 or 3 mM $Mg(OAc)_2$ (Figure 4, MS lanes) or in 50 mM HEPES-KOH (pH 8), 800 mM NH_4OAc, and 2 or 3 mM $MgCl_2$ (Figure 4, PRA lanes), the activity is similar and shows the expected substrate cleavage specificity; without the RPPs, the RPR is not active in 2 or 3 mM Mg^{2+} (data not shown). These results indicate that a functional *Pfu* RNase P is assembled under conditions identical to those used in the MS studies.

Having determined the subunit stoichiometry of the 4-RPP *Pfu* RNase P complex, we next explored assembly intermediates en route to this final RNP. Although the RPR

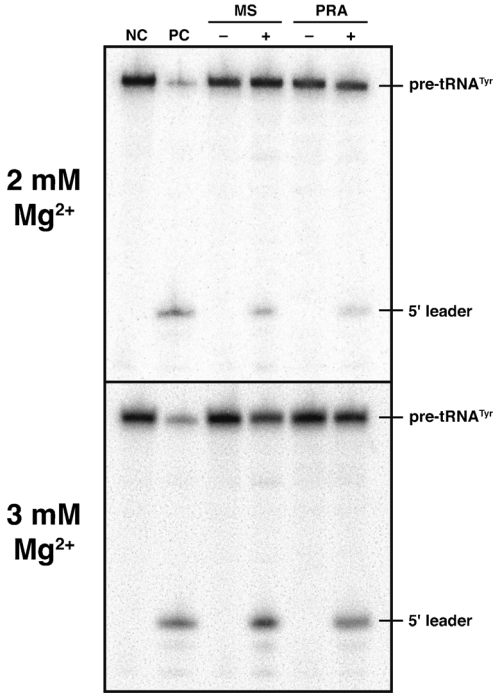

Figure 4. Comparison of the pre-$tRNA^{Tyr}$ processing activity at 55 °C of the 4-RPP *Pfu* RNase P complex reconstituted in vitro under conditions employed for native MS (MS) and those previously optimized for function in vitro (PRA).[10a,d] NC, a negative control with pre-$tRNA^{Tyr}$ alone; PC, a positive control with in vitro reconstituted *Escherichia coli* RNase P and pre-$tRNA^{Tyr}$; – and + are parallel reactions performed without and with *Pfu* RNase P, respectively. See the Supporting Information for additional details.

is active without its cognate RPPs in 500 mM Mg^{2+}, its activity is significantly increased by RPP21·RPP29 or POP5·RPP30 at lower substrate and Mg^{2+} concentrations. That RPR + RPP21·RPP29 and RPR + POP5·RPP30 constitute minimal functional complexes is evident from their k_{cat}/K_M values that are, respectively, 8- to 80-fold higher than the RPR alone and 600- to 50-fold lower than the RPR with both binary RPPs.[10d] These partial complexes exhibited the highest activity in 50 mM Tris-HCl/HEPES-KOH (pH 7.5–8), 100 mM NH_4OAc, and 120 mM $MgCl_2$. Here we also determined the optimal conditions that would permit assembly and native MS studies. Based on the premise that most of the 120 mM Mg^{2+} used in the activity assays served as counterions to aid the native RNA/RNP fold, we proportionately increased NH_4OAc from 100 to 500 mM to compensate for the decreased ionic strength associated with lowering the Mg^{2+} concentration.

We then determined the stoichiometry of *Pfu* RPR + RPP21·RPP29 and RPR + POP5·RPP30 complexes in 500 mM NH_4OAc with varying $Mg(OAc)_2$ concentrations. In 10 mM $Mg(OAc)_2$, RPP21·RPP29 binds the RPR to generate a complex with a mass consistent with either RPR + RPP21·RPP29, RPR + $(RPP21)_2$, or RPR + $(RPP29)_2$, an ambiguity resulting from the similar masses of RPP21 and RPP29 (Figure 5a; Table S1). Of these, the first complex is the most likely based on the strong interaction between RPP21 and RPP29 as revealed in high-resolution structures,[11a,d] and the finding that the RPR is activated by RPP21·RPP29, but not by either RPP21 or RPP29.[10d] We attribute the 2.7 kDa difference between our experimentally determined value and the predicted mass (Table S1) to severe peak broadening caused by the 10 mM $Mg(OAc)_2$ required for generating this RNP complex. Even with optimization of the collision-induced cleaning voltage, exceeding a certain Mg^{2+} threshold clearly poses a problem for MS analysis.

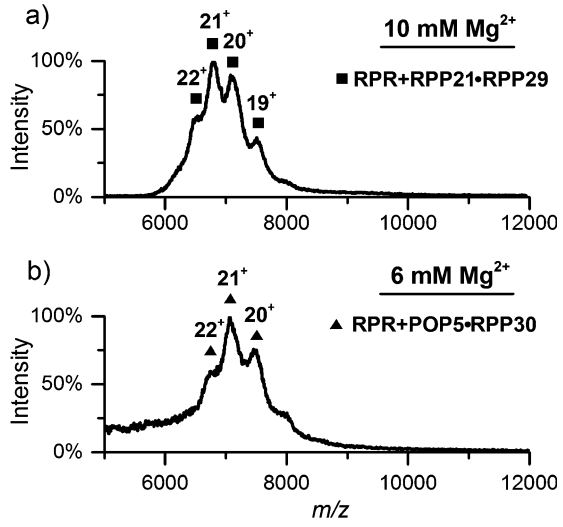

Figure 5. a) RPR and RPP21·RPP29 in 500 mM NH_4OAc and 10 mM $Mg(OAc)_2$. b) RPR and POP5·RPP30 in 500 mM NH_4OAc and 6 mM $Mg(OAc)_2$. In both, (a) and (b), the dominant peaks correspond to the RPR bound to one copy of the respective binary RPP complex. Collision-induced cleaning was used to partially remove nonspecific adducts, providing better resolved peaks with optimal collision voltage at 110 V (see Figure S2 for a more detailed analysis of panel (b)).

POP5·RPP30 binds the RPR in 6 mM $Mg(OAc)_2$ to form RPR + POP5·RPP30 (Figure 5b), but forms a $(POP5·RPP30)_2$ heterotetramer under identical conditions without RPR (data not shown). The abrupt structural change by POP5·RPP30 in the presence of the RPR with or without RPP21·RPP29 motivated us to examine possible intermediates. After considerable effort, we found that when POP5·RPP30 was assembled with RPR in 500 mM NH_4OAc and 4 mM $Mg(OAc)_2$, IM could be used to extract minor signals corresponding to RPR + $(POP5·RPP30)_2$ from background noise and other interference (Figure S2b). However, when the $Mg(OAc)_2$ concentration was increased from 4 to 6 mM, which is more favorable for RNase P activity, RPR + POP5·RPP30 is the only species observed (Figures 5b and S2d); this was the case even with a two-fold excess of RPPs over RPR (data not shown). Although present, the significance of the low-abundance, RNA-bound heterotetramer at 4 mM $Mg(OAc)_2$ is unclear. These data suggest that tight RPR binding is concomitant with a disruption of this heterotetramer (Figure S3).

Based on functional assays, we had proposed that the assembly of *Pfu* RPR with RPP21·RPP29 and POP5· RPP30 entails binding of either RPP complex to the RPR followed by binding of the other.[10d] Under the conditions used for MS, RPP21·RPP29 requires at least 10 mM Mg^{2+}, whereas POP5·RPP30 binds the RPR in as little as 6 mM Mg^{2+}. These findings suggest that POP5·RPP30 may be the first to assemble with the RPR at cellular Mg^{2+} concentration (< 2 mM).[19]

Although the stoichiometry and oligomeric state of the archaeal/eukaryal RNase P have not been previously determined experimentally, the expectation that RPPs might be present in multiple copies, in contrast to our finding of single copies, was based on at least three lines of evidence. First, in the absence of the RPR, crystallographic and NMR studies revealed a $(POP5·RPP30)_2$ heterotetramer[11b,c,13] (now confirmed in the gas phase; Figure 1). Although data were not shown, the deletion of a loop in *Pho* POP5 was reported to render it defective in homodimerization and to abolish *Pho* RNase P activity;[11b] because this mutant could only form POP5·RPP30 and not $(POP5·RPP30)_2$, tetramer formation was inferred as essential for activity. However, a defect in this mutant's ability to bind RPR could also impair its activity, an untested premise. Second, an EM study on yeast RNase P and MRP (a sister RNP enzyme to RNase P that requires most of the RPPs for function) suggests the presence of two copies of RPP30, one bound to POP5 and another to RPP14 (a POP5 homolog).[20] Finally, the staining of native preparations of yeast RNase P and MRP suggests greater amounts of some RPPs than of others,[21] though the bias of gel stains for some protein compositions imparts uncertainty to this argument. In contrast, the mass determined by native MS provides evidence for only one RPR and one of each RPP in both 4- and 2-RPP *Pfu* RNase P complexes, the most definitive stoichiometry of an active RNase P to date.

Taken together, our study illustrates the value of collision-induced cleaning and native tandem SID coupled with IM-MS

for improved peak resolution, confirmation of subunit composition, and parsing conformational heterogeneity of a Mg^{2+}-containing RNA-protein complex. It is a valuable structural biology tool that can provide insights into the structure and dynamics of large RNA–protein complexes, which might be refractory to other high-resolution methods.

Received: May 16, 2014
Revised: July 16, 2014
Published online: September 4, 2014

Keywords: ion mobility · native mass spectrometry · RNA–protein complexes · RNase P · stoichiometry · surface-induced dissociation

[1] a) H. Hernández, C. V. Robinson, *Nat. Protoc.* **2007**, *2*, 715 – 726; b) J. L. P. Benesch, B. T. Ruotolo, D. A. Simmons, C. V. Robinson, *Chem. Rev.* **2007**, *107*, 3544 – 3567; c) C. S. Kaddis, S. H. Lomeli, S. Yin, B. Berhane, M. I. Apostol, V. A. Kickhoefer, L. H. Rome, J. A. Loo, *J. Am. Soc. Mass Spectrom.* **2007**, *18*, 1206 – 1216; d) C. S. Kaddis, J. A. Loo, *Anal. Chem.* **2007**, *79*, 1778 – 1784; e) A. J. R. Heck, *Nat. Methods* **2008**, *5*, 927 – 933; f) A. J. R. Heck, R. H. H. van den Heuvel, *Mass Spectrom. Rev.* **2004**, *23*, 368 – 389; g) C. N. Pace, S. Treviño, E. Prabhakaran, J. M. Scholtz, *Philos. Trans. R. Soc. London Ser. B* **2004**, *359*, 1225 – 1235; h) B. T. Ruotolo, J. L. P. Benesch, A. M. Sandercock, S.-J. Hyung, C. V. Robinson, *Nat. Protoc.* **2008**, *3*, 1139 – 1152; i) C. Uetrecht, N. R. Watts, S. J. Stahl, P. T. Wingfield, A. C. Steven, A. J. R. Heck, *Phys. Chem. Chem. Phys.* **2010**, *12*, 13368 – 13371; j) G. K. Shoemaker, E. van Duijn, S. E. Crawford, C. Uetrecht, M. Baclayon, W. H. Roos, G. J. L. Wuite, M. K. Estes, B. V. V. Prasad, A. J. R. Heck, *Mol. Cell. Proteomics* **2010**, *9*, 1742 – 1751; k) C. Uetrecht, I. M. Barbu, G. K. Shoemaker, E. van Duijn, A. J. R. Heck, *Nat. Chem.* **2011**, *3*, 126 – 132; l) C. Uetrecht, A. J. R. Heck, *Angew. Chem. Int. Ed.* **2011**, *50*, 8248 – 8262; *Angew. Chem.* **2011**, *123*, 8398 – 8413.

[2] a) A. J. Callaghan, J. G. Grossmann, Y. U. Redko, L. L. Ilag, M. C. Moncrieffe, M. F. Symmons, C. V. Robinson, K. J. McDowall, B. F. Luisi, *Biochemistry* **2003**, *42*, 13848 – 13855; b) B. T. Ruotolo, K. Giles, I. Campuzano, A. M. Sandercock, R. H. Bateman, C. V. Robinson, *Science* **2005**, *310*, 1658 – 1661; c) S. Akashi, M. Watanabe, J. G. Heddle, S. Unzai, S.-Y. Park, J. R. H. Tame, *Anal. Chem.* **2009**, *81*, 2218 – 2226.

[3] a) R. King, R. Bonfiglio, C. Fernandez-Metzler, C. Miller-Stein, T. Olah, *J. Am. Soc. Mass Spectrom.* **2000**, *11*, 942 – 950; b) T. M. Annesley, *Clin. Chem.* **2003**, *49*, 1041 – 1044.

[4] a) P. F. Crain, J. A. McCloskey, *Curr. Opin. Biotechnol.* **1998**, *9*, 25 – 34; b) J. Pan, K. Xu, X. Yang, W.-Y. Choy, L. Konermann, *Anal. Chem.* **2009**, *81*, 5008 – 5015.

[5] U. H. Verkerk, P. Kebarle, *J. Am. Soc. Mass Spectrom.* **2005**, *16*, 1325 – 1341.

[6] a) Z. Hall, C. V. Robinson, *J. Am. Soc. Mass Spectrom.* **2012**, *23*, 1161 – 1168; b) E. Jurneczko, P. E. Barran, *Analyst* **2011**, *136*, 20 – 28; c) H. Borsdorf, T. Mayer, M. Zarejousheghani, G. A. Eiceman, *Appl. Spectrosc. Rev.* **2011**, *46*, 472 – 521.

[7] L. B. Lai, I.-M. Cho, W.-Y. Chen, V. Gopalan in *Ribonuclease P* (Eds.: F. Liu, S. Altman), Springer, New York, **2010**, pp. 153 – 172.

[8] W. Rossmanith, *Biochim. Biophys. Acta Gene Regul. Mech.* **2012**, *1819*, 1017 – 1026.

[9] a) L. B. Lai, A. Vioque, L. A. Kirsebom, V. Gopalan, *FEBS Lett.* **2010**, *584*, 287 – 296; b) S. C. Walker, D. R. Engelke, *Crit. Rev. Biochem. Mol. Biol.* **2006**, *41*, 77 – 102.

[10] a) W.-Y. Chen, D. K. Pulukkunat, I.-M. Cho, H.-Y. Tsai, V. Gopalan, *Nucleic Acids Res.* **2010**, *38*, 8316 – 8327; b) I.-M. Cho, L. B. Lai, D. Susanti, B. Mukhopadhyay, V. Gopalan, *Proc. Natl. Acad. Sci. USA* **2010**, *107*, 14573 – 14578; c) Y. Kouzuma, M. Mizoguchi, H. Takagi, H. Fukuhara, M. Tsukamoto, T. Numata, M. Kimura, *Biochem. Biophys. Res. Commun.* **2003**, *306*, 666 – 673; d) H.-Y. Tsai, D. K. Pulukkunat, W. K. Woznick, V. Gopalan, *Proc. Natl. Acad. Sci. USA* **2006**, *103*, 16147 – 16152.

[11] a) T. Honda, Y. Kakuta, K. Kimura, J. Saho, M. Kimura, *J. Mol. Biol.* **2008**, *384*, 652 – 662; b) S. Kawano, T. Nakashima, Y. Kakuta, I. Tanaka, M. Kimura, *J. Mol. Biol.* **2006**, *357*, 583 – 591; c) R. C. Wilson, C. J. Bohlen, M. P. Foster, C. E. Bell, *Proc. Natl. Acad. Sci. USA* **2006**, *103*, 873 – 878; d) Y. Xu, C. D. Amero, D. K. Pulukkunat, V. Gopalan, M. P. Foster, *J. Mol. Biol.* **2009**, *393*, 1043 – 1055.

[12] a) T. A. Hall, J. W. Brown, *Archaea* **2004**, *1*, 247 – 254; b) M. Kifusa, H. Fukuhara, T. Hayashi, M. Kimura, *Biosci. Biotechnol. Biochem.* **2005**, *69*, 1209 – 1212.

[13] B. L. Crowe, C. J. Bohlen, R. C. Wilson, V. Gopalan, M. P. Foster, *Archaea* **2011**, DOI: 10.1155/2011/891531.

[14] a) E. O. Hochleitner, B. Kastner, T. Fröhlich, A. Schmidt, R. Lührmann, G. Arnold, F. Lottspeich, *J. Biol. Chem.* **2005**, *280*, 2536 – 2542; b) D. E. Agafonov, J. Deckert, E. Wolf, P. Odenwälder, S. Bessonov, C. L. Will, H. Urlaub, R. Lührmann, *Mol. Cell. Biol.* **2011**, *31*, 2667 – 2682; c) C. Schmidt, M. Grønborg, J. Deckert, S. Bessonov, T. Conrad, R. Lührmann, H. Urlaub, *RNA* **2014**, *20*, 406 – 420.

[15] H. Borsdorf, G. A. Eiceman, *Appl. Spectrosc. Rev.* **2006**, *41*, 323 – 375.

[16] a) N. Morgner, F. Montenegro, N. P. Barrera, C. V. Robinson, *J. Mol. Biol.* **2012**, *423*, 1 – 13; b) A. J. Borysik, C. V. Robinson, *Phys. Chem. Chem. Phys.* **2012**, *14*, 14439 – 14449; c) J. L. P. Benesch, *J. Am. Soc. Mass Spectrom.* **2009**, *20*, 341 – 348; d) A. R. McKay, B. T. Ruotolo, L. L. Ilag, C. V. Robinson, *J. Am. Chem. Soc.* **2006**, *128*, 11433 – 11442.

[17] a) L. Han, S.-J. Hyung, B. T. Ruotolo, *Angew. Chem. Int. Ed.* **2012**, *51*, 5692 – 5695; *Angew. Chem.* **2012**, *124*, 5790 – 5793; b) L. Han, S.-J. Hyung, B. T. Ruotolo, *Faraday Discuss.* **2013**, *160*, 371 – 388; c) L. Han, B. T. Ruotolo, *Angew. Chem. Int. Ed.* **2013**, *52*, 8329 – 8332; *Angew. Chem.* **2013**, *125*, 8487 – 8490; d) J. Liu, L. Konermann, *J. Am. Soc. Mass Spectrom.* **2014**, *25*, 595 – 603.

[18] a) F. M. Fernandez, V. H. Wysocki, J. H. Futrell, J. Laskin, *J. Am. Soc. Mass Spectrom.* **2006**, *17*, 700 – 709; b) V. H. Wysocki, K. E. Joyce, C. M. Jones, R. L. Beardsley, *J. Am. Soc. Mass Spectrom.* **2008**, *19*, 190 – 208; c) V. H. Wysocki, C. M. Jones, A. S. Galhena, A. E. Blackwell, *J. Am. Soc. Mass Spectrom.* **2008**, *19*, 903 – 913; d) R. L. Beardsley, C. M. Jones, A. S. Galhena, V. H. Wysocki, *Anal. Chem.* **2009**, *81*, 1347 – 1356.

[19] J. A. Cowan in *The Biological Chemistry of Magnesium* (Ed.: J. A. Cowan), VCH Publishers, New York, **1995**, pp. 1 – 23.

[20] K. Hipp, K. Galani, C. Batisse, S. Prinz, B. Bottcher, *Nucleic Acids Res.* **2012**, *40*, 3275 – 3288.

[21] K. Salinas, S. Wierzbicki, L. Zhou, M. E. Schmitt, *J. Biol. Chem.* **2005**, *280*, 11352 – 11360.

